Turbulence Effect on Direct-Contact Heat Transfer with Change of Phase:

Effect of Mixing on Heat Transfer between an Evaporating Volatile Liquid in Direct Contact with an Immiscible Liquid Medium

SAMUEL SIDEMAN and ZVI BARSKY

Israel Institute of Technology, Haifa, Israel

The concept of local isotropy in turbulent agitation together with the particular characteristics of volatile drops evaporating while in dispersion were used to derive a simple and practical correlation relating the specific power input with the temperature driving force and the heat flow rates for all conceivable mixing regimes. The correlation was verified by experiments which indicate that dilute evaporating dispersions are controlled by viscous shear stresses.

The generality of the proposed correlation is demonstrated by its application to pilot plant and laboratory data obtained over a wide range of turbulent mixing intensities. At its lower limit the correlation reduces to the well-known relationship of surface-boiling heat transfer.

Direct-contact heat transfer between a volatile dispersed phase evaporating into the continuous phase is a relatively new mode of heat transfer operation. It is at present mainly associated with water desalination projects based on direct-contact freezing. Apart from the usual advantages of direct-contact operations under dispersion (high transfer area per unit volume, uniform driving forces, and absence of scale), this technique permits appreciably low mass flow of the coolant, lower temperature gradients between the phases, and convenient continuous separation of the phases; its transfer coefficients are one order of magnitude higher compared with nonevaporating systems (*1*).

The object of this work was a general and simple relationship between the energy input and turbulence in the mixing apparatus, the temperature driving force, and the heat flow rate for the three-phase two-component system. In deriving this relationship, use was made of the well-known two-phase correlations for liquid-liquid and liquid-gas systems, as well as of the particular characteristics of volatile drops and layers evaporating by direct contact with another immiscible liquid.

For the sake of completeness, the established mixing theories used in this work are briefly reviewed.

MIXING REGIMES FOR LIQUID-LIQUID AND LIQUID-GAS SYSTEMS

Different mixing correlations are obtained when one operates under different mixing regimes (*2, 3*). This explains the wide variety of contradictory mixing correlations proposed in literature, sometimes on the basis of apparently similar systems.

When two immiscible fluids are agitated, a dispersion is formed in which continuous breakup and coalescence of droplets (or bubbles) occur simultaneously. The average size of the droplets at equilibrium then depends on the conditions of agitation and physical properties of the components. Drops and bubbles may be broken up by viscous shear forces, especially near the agitator blades, as well as by turbulent velocity (kinetic energy) and pressure variation along the surface of a single particle. In addition, turbulent flow may accelerate or slow down coalescence of the droplets (*3*). Whereas the first phenomenon usually predominates in dilute dispersions, prevention of coalescence by turbulence generally controls in cases of concentrated dispersions susceptible to coalescence. Thus, except for high shear regimes, the particle diameter is determined by the local flow characteristics around and past it, with relatively little effect of the large-scale flow patterns in the mixing apparatus. Or, as suggested by Kolmogoroff (*4*), the statistical properties of the flow field (the small scale components of the turbulent velocity fluctuations) in a very small volume of liquid in which turbulence is locally isotropic are independent of the main flow of the turbulence-generating mechanism, provided the Reynolds numbers are sufficiently high. Thus, in accordance with this local isotropy hypothesis, the small scale velocity fluctuations are determined by the local rate of energy dissipation per unit mass of fluid ϵ and the kinematic viscosity ν. Each small-scale eddy is defined by a length scale

$$\eta = (\nu^3/\epsilon)^{0.25} \tag{1}$$

and a velocity scale

$$v = (\nu\epsilon)^{0.25} \tag{2}$$

which can be used to define the conditions of flow. For local isotropy to exist, the linear scale L (which is of the order of magnitude of the width of the blades) of the energy-containing eddies must be large compared with η, that of the small energy-dissipating eddies. All velocity correlations in any small volume of characteristic dimension r ($<< L$) must then be functions of η and v (or ν and ϵ) only. The mean square of the relative velocity $\overline{u^2(r)}$ between any two points a distance r apart is a uni-

Zvi Barsky is with the Ministry of Development, Jerusalem, Israel.

versal function of η and v. Furthermore, if $L >> r >> \eta$, then $\overline{u^2(r)}$ is independent of viscosity.

The universal function is obtainable by dimensional analysis. Thus

$$\overline{u^2(r)} = C_1(\epsilon r)^{2/3}; \quad L >> r >> \eta \tag{3}$$

$$\overline{u^2(r)} = C_2(\epsilon r^2/\nu); \quad L >> \eta >> r \tag{4}$$

In other words, at high enough Reynolds numbers under local isotropic turbulence the ratio of the mean velocity for any two points is independent of the Reynolds number (defined as ND^2/ν). This is consistent with the findings of Aiba (5), who showed experimentally that at $Re > 10^4$ the velocity components in mixing vessels are identical irrespective of the type of mixer used and that the velocity ratio for any two points is independent of the velocity of the mixer.

The theory of local isotropy is closely related to the criterion of specific power input commonly used for mixing equipment scale up from experimental results. Rushton et al. (6) showed that at high Reynolds numbers $\bar{\epsilon}$, the energy input of the mixing impeller per unit mass of liquid, is independent of the properties of the liquid and a function of the geometric scale of the impeller D and its speed N.

In addition, under conditions of local isotropy and universal velocity distribution, the local rate of energy dissipation ϵ is independent of space and directly proportional to $\bar{\epsilon}$. Thus (6, 3)

$$\epsilon(x, y, z) = K^1\bar{\epsilon} = KN^3D^2 \tag{5}$$

Whereas Rushton (6) obtained Equation (5) for single-phase mixing, Vermeulen et al. (7) showed it is also valid for heterogeneous systems.

The three main mixing regimes may now be summarized (2, 3).

Viscous Shear Regime

Particle breakup is mainly in the high shear regime when interfacial tension σ is very low or the kinematic viscosity ν rather high. The particle diameter d is smaller than the linear scale η of the small-scale eddies. In this case

$$\frac{\rho_c \nu_c^{1/2}\bar{\epsilon}^{1/2}}{\sigma} d = f\left(\frac{\mu_d}{\mu_c}\right) \tag{6}$$

substitution of (5) in (6) yields

$$N_{Re}^{-1/2} N_{We} \frac{d}{D} = f\left(\frac{\mu_d}{\mu_c}\right) \tag{7}$$

Kinetic Energy Regime

Particle breakup is mainly due to fluctuations in the local turbulent velocity and pressure variation along the particle surface. At $d >> \eta$ viscous forces are negligible. In this case the kinetic energy of the oscillations balances the surface energy gains owing to breakup, and

$$\frac{\rho_c \bar{\epsilon}^{2/3} d^{5/3}}{\sigma} = \text{const} \tag{8}$$

Substitution of (5) in (8) yields the well-known relationship

$$\frac{d}{D} \sim N_{We}^{-0.6} \tag{9}$$

Coalescence Prevention Regime

Local velocity fluctuation accelerates or slows down coalescence of the dispersed particles, depending upon adhesion forces and $\bar{\epsilon}$, the intensity of turbulence. On the basis of the fact that adhesion and inertial forces are different functions of the particle diameter, Shinnar and Church (2) obtained

$$\rho_c \bar{\epsilon}^{2/3} d^{5/3} = \text{const} \tag{10}$$

or

$$\rho_c N^2 D^{4/3} d^{5/3} = \text{const} \tag{11}$$

Some of the relevant empirical results reported in literature may now be reviewed. For liquid-gas systems Vermeulen et al. (8) obtained results in agreement with Equation (7), viscous forces controlling. Calderbank (9), however, obtained an equation which apparently points to the kinematic breakup regime controlling liquid-gas systems. However, when one considers the dependence of the gas holdup term in his equation on some of the factors affecting the mixing process [see Equation (16)], his equation may be rewritten so as to indicate that the coalescence regime is the controlling one. This conclusion is consistent with the fact that the particle diameter in his system was determined by the nozzle diameter and with his remarks as to the presence of coalescence. Correlations for liquid-liquid systems (8, 9, 10, 11) seem to indicate a kinetic breakup regime. With higher liquid ratios (50 to 50%), Rodger et al. (12) obtained results indicating the predominance of the coalescence-prevention regime.

It should be noted that Equations (6) and (8) were derived for low holdups of the dispersed phase under the assumption of no interaction between the dispersed particles. However, experiments (8, 9, 10) showed a dependence of the average particle diameter on the dispersed phase holdup ϕ. According to Vermeulen (8), the same dependence prevails in liquid-liquid and liquid-gas systems. Based on experimental evidence one can assume that the effect of holdup on particle diameter is negligible at holdup below 5%. At higher holdups the following relationship is assumed on the basis of experimental work (8, 9, 10):

$$d \sim \phi^{0.6} \tag{12}$$

Substitution of Equation (12) in (6) and (8) yields, for the viscous regime

$$\rho_c \nu_c^{1/2}\bar{\epsilon}^{1/2}\phi^{-0.6} d/\sigma = f(\mu_d/\mu_c) \tag{13}$$

and for the kinetic regime

$$\rho_c \bar{\epsilon}^{2/3} d^{5/3}\phi^{-1.0}/\sigma = \text{const} \tag{14}$$

EFFECT OF EVAPORATION RATE ON POWER INPUT

The rate of evaporation of the volatile dispersed phase in the three-phase system treated here determines the rates of vapor generation in the systems. This affects the power input, which in turn affects the particle diameter. In its extreme case, the dispersion undergoes partial breakup with increasing gas load (all other conditions being constant), and a layer of the lighter volatile liquid (in this case pentane) forms on top of the bubbling dispersion.

The effect of gas flow in mixing vessels was studied (13, 14, 15, 17) in connection with fermentation processes. Introduction of air into the mixing apparatus, operating in the turbulent regime, resulted in an apreciable drop in power input entirely unrelated to the decrease in the average density of the fluids. A 75% decrease in power input was observed for a mere 5% decrease in average density (13, 14). This may be due to the fact that gas accumulates around the blades and effectively isolates them from the main body of fluids. (This explanation is substantiated by the fact that under the same operating conditions the

TABLE 1. CONSTANTS FOR EQUATION (15)

Mixer	No. of blades	a	b	Ref.
Vaned disk	2	30	1	(16)
Vaned disk	4	20	1	(16)
Vaned disk	6	10	1	(16)
Vaned disk	8	1.77	0.55	(16)
Vaned disk	8	1.62	0.5	(17)
Paddle	2	18	1	(16)
Turbine	6	12.1	1	(9)
Turbine	8	2.29	0.69	(16)

TABLE 2. CONSTANTS FOR EQUATION (15a)

Mixer	No. of blades	a'	b'	Ref.
Vaned disk	2	0.35	1.1	(16)
Vaned disk	4	0.35	1.1	(16)
Vaned disk	6	0.40	1.1	(16)
Vaned disk	8	0.50	1.1	(16)
Paddle	2	0.37	1.15	(16)
Turbine	6	0.62	1.85	(9)
Turbine	8	0.40	0.28	(16)

effect of the gas varies with impeller design and is larger than the closer the impeller.)

As the relative density differential in different liquid-gas systems is rather small, it may be assumed that similar relationships will hold for different gas-liquid systems. Moreover, the effect of gas on the mixing power input was found (15, 16) to be independent of the mode of gas introduction. It may thus be expected that, regardless of the fact that in the authors' system the vapor is generated during the mixing process, the behavior of the water-vapor system would be quite similar to the established characteristics of liquid-air systems.

As already stated, the effect of the gas depends on the type and design of the agitator. This effect may be expressed in terms of a dimensionless group representing the ratio of the gas and mixer flow rates (14, 16, 17). Accordingly

$$\frac{\bar{\epsilon}}{\bar{\epsilon}_o} = 1 - a\left(\frac{G}{ND^3}\right)^b \qquad (15)$$

The constants, derived from the experiment curves of Oyama and Endoh (16), are summarized in Table 1.

A slightly modified form of Equation (15) is used for operation beyond the flooding point of the mixer, defined as the point where power input falls below 35% of its value in the absence of gas:

$$\frac{\bar{\epsilon}}{\bar{\epsilon}_o} = a' - b'\left(\frac{G}{ND^3}\right) \qquad (15a)$$

The constants a' and b', as derived from (16) are summarized in Table 2.

As is to be expected, the gas holdup (and residence time) is dependent on the power input. The suggested (9) relationship between gas holdup ϕ_G, power input per unit fluid volume P/V, and gas flow rate is

$$\phi_G \sim \left(\frac{P}{V}\right)^{0.4}\left(\frac{G}{D^2}\right)^{0.5} \qquad (16)$$

A similar relationship is also reported by Rushton et al. (18).

HEAT TRANSFER COEFFICIENT

The volatile fluid normally enters the mixing vessel at or very close to its boiling point, and it may be assumed that all the heat transferred to the droplet serves to increase its vapor content. In other words, the heat flow to the drops is proportional to G, the gas flow rate defined above.

In earlier studies of evaporating drops in immiscible liquid media (1), the heat transfer coefficient increased from nonevaporating drop values (about 0.01 cal./sec./sq. cm./°C. to evaporating drop values (about 0.1 cal./sec./sq. cm./°C.) when only some 3 to 5 wt. % of the volatile liquid evaporated, remaining practically constant throughout the rest of the evaporation process. Thus, whereas the internal resistance controls the transfer mechanism in the first evaporation stages, it may be assumed to be negligible compared with the external resistance during most of the evaporation process. Moreover, the mixing apparatus under steady state conditions would contain drops with different vapor contents. Since the rate of heat transfer to the droplets with low vapor content is relatively small compared with the other evaporating droplets, it may be assumed that the heat transferred to the former droplets is small and practically negligible compared with the overall heat flow in the mixer. The negligibility of the internal resistance to heat transfer is consistent with the observed thinning of the volatile liquid layer at the bottom of the evaporating droplets at vapor contents above 1% (wt.).

Film resistance in the continuous phase enclosing the drops and bubbles is treated extensively in literature (19, 20). The familiar formula relating the film heat transfer coefficient h to the various variables involved is

$$\frac{hd}{k_c} \sim \left(\frac{C_p\mu}{k}\right)_c^{\alpha}\left(\frac{du}{\nu_c}\right)^{\beta} \qquad (17)$$

u may be given by Equations (3) and (4), depending on the system and flow characteristics. For the kinetic regime or that of coalescence prevention by turbulent flow, substitution of (3) in (17) yields

$$\frac{hd}{k_c} \sim \left(\frac{C_p\mu}{k}\right)_c^{\alpha}\left(\frac{d^{4/3}\bar{\epsilon}^{1/3}}{\nu_c}\right)^{\beta} \qquad (18)$$

Similarly, for the viscous regimes, substitution of (4) in (17) yields

$$\frac{hd}{k_c} \sim \left(\frac{C_p\mu}{k}\right)_c^{\alpha}\left(\frac{d^2\bar{\epsilon}^{1/2}}{\nu_c^{3/2}}\right)^{\beta} \qquad (19)$$

As shown by Calderbank and Moo-Young (20) and others (19, 21), the continuous phase transfer coefficient is practically independent of particle size within the approximate size ranges of $d < 2$-3 and $d > 3$ mm. Calderbank and Moo-Young (20) have also shown that $h_c \sim k^{2/3}$ for turbulently mixed systems where particle diameter is less than 2.5 mm. Obviously, the average diameter of the particles in turbulent flow, where conditions for local isotropy exist, will most probably be less than 1 mm. Thus, if the above relationships are assumed to hold, one gets $\alpha = 1/3$, $\beta = 1/2$ for the viscous regime and $\alpha = 1/3$, $\beta = 3/4$ for the kinetic and coalescence prevention regime. (It is noteworthy that Barker and Treybal (21) have found the mass transfer coefficient in solid-liquid systems to be independent of the Schmidt number which, by analogy, would yield $\alpha = 1$.) These results are consistent with the well-known dependence of N_{Nu} on $(N_{Re})^{0.6}$ mixer. Substitution of these values in Equations (18) and (19) yields, for a given system

$$h \sim \bar{\epsilon}^{1/4} \tag{20}$$

indicating that the heat transfer coefficient is independent of the mixing regime. This important conclusion is not surprising in view of the independence of the transfer coefficient of the particle diameter in this range size. Recalling the assumption of internal negligible resistance, we may now write

$$U \sim \bar{\epsilon}^{1/4} \tag{21}$$

EFFECTIVE HEAT TRANSFER AREA

The effective heat transfer area is limited to the liquid-liquid interface (*1*). Experiments (*1*) showed that, within experimental error and in the relatively low range of temperature differences studied (up to 14°C.)

$$U \neq f(\Delta T) \tag{21}$$

and as already stated

$$U \neq f(m) \tag{22}$$

where m is the vapor content in the evaporating droplet in weight fraction. A study of consecutive cine-camera pictures taken during the evaporation process indicated that

$$m \sim t^3 \tag{23}$$

Since $U \cong$ constant and $\Delta T \simeq$ constant for a given system

$$q \sim A \sim \frac{dm}{dt} \sim m^{2/3} \tag{24}$$

Under the conditions of turbulent mixing, where particle size is rather small, it may be assumed that the two-phase particle remains spherical with the gaseous phase concentrated at the top. The heat transfer area is then a function of the particle size and vapor content. These two parameters may be considered as practically independent, since the particle diameter depends mainly on the mixing power input. Thus, since $d \neq f(m)$ in this case

$$A \sim f(d, m) \sim d^2 m^{2/3} \tag{25}$$

and the effective heat transfer area per unit volume of fluid is given by

$$A_v \sim \frac{d^2}{d^3} \phi\, m^{2/3} \tag{26}$$

As can easily be shown, above 3% (wt.) vapor content, the volume of the volatile liquid in the two-phase particle is negligible compared with the volume of the gaseous phase, and $\phi \simeq \phi_G$. Thus, the relationship between the dispersed phase holdup (volumetric) and m is given by

$$m = \frac{[\text{weight of gas}]}{[\text{total weight of liquid phase}]} = \frac{\phi_G \rho_G}{\phi_o \rho_o} \tag{27}$$

where ϕ_o and ρ_o denote holdup and density of the non-evaporating dispersed phase. For a steady state definite system ϕ_o is constant, and

$$m \sim \phi_G \tag{28}$$

$$A_v \sim \phi_G^{5/3}/d \tag{29}$$

Substituting Equation (16) in (29) and referring to Equation (36) one obtains

$$A_v \sim \bar{\epsilon}^{4/6} q_v^{5/6}/d \tag{30}$$

THE DERIVED CORRELATION FOR THE LIQUID-(EVAPORATING) LIQUID SYSTEM

For the case of $\phi < 5\%$, where each droplet evaporates completely while still in dispersion and all other previously made assumptions still hold, substitution of Equations (30) and (20*a*) in the general heat transfer equation

$$q_v = U A_v \Delta T \tag{31}$$

yields the average particle size as function of the specific power input, temperature difference, and heat flow rate:

$$d \sim \frac{\bar{\epsilon}^{11/12} \Delta T}{q_v^{1/6}} \tag{32}$$

For a specific system of constant properties, substitution of Equation (32) in Equations (6), (8), and (10) yields

$$\frac{q_v^{1/6}}{\Delta T} \sim \bar{\epsilon}^{y} \tag{33}$$

where the value of the exponent 'y' is $y = 17/12$ for the viscous breakup regime, $y = 79/60$ for the kinetic breakup regime, and $y = 7/6$ for the coalescence prevention regime.

It is noted that $\bar{\epsilon}$ may be determined from Equation (15) whenever it is not directly measurable. This, however, requires knowledge of the constants a and b, Equation (15), as well as of the vapor flow rate (the latter being obviously directly measurable). Thus, for a given system, the variables involved are q_v and ΔT, which are usually dictated by the process requirements with N and D as dependent variables.

EXPERIMENTAL VERIFICATION OF THE DERIVED CORRELATION

Apparatus and Experimental Procedure

The schematic diagram of the experimental setup is shown in Figure 1. The mixing cell, 212 mm. I.D. and 210 mm. high was made of glass with four baffles 20 mm. wide. The electrically-heated bottom was of chrome-plated copper with two thermocouples embedded and flush with the surface (before plating). The top was provided with a 2-cm. diameter connection to a vertical water-cooled condenser. A four-blade paddle mixer, 70 mm. diameter and 12 mm. wide, was set 70 mm. above the bottom. A special sealing device was provided against vapor leakage. A reduction gear was used whenever necessary, and the shaft speed, controlled by a variac, was measured directly by a tachometer. The cell was completely insulated except for two narrow vertical slits for visual observation. Temperatures in the cell were measured by two copper-constantan thermocouples, 7 cm. apart, and an immersed glass mercury thermometer. The electric heat load and the cooling water flow rates and temperatures were measured (average deviation 4%), the former being used as the actual heat load.

n-penpane was used as the dispersed phase, and tap water was the continuous phase. Red coloring matter was added to the pentane to facilitate observation. The cell contained 5 liters of water, and pentane was added to form a 5% (vol-

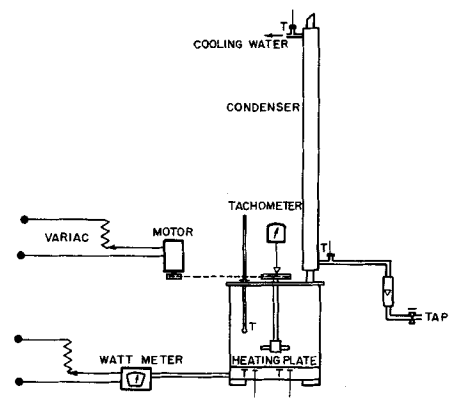

Fig. 1. Schematic diagram of apparatus.

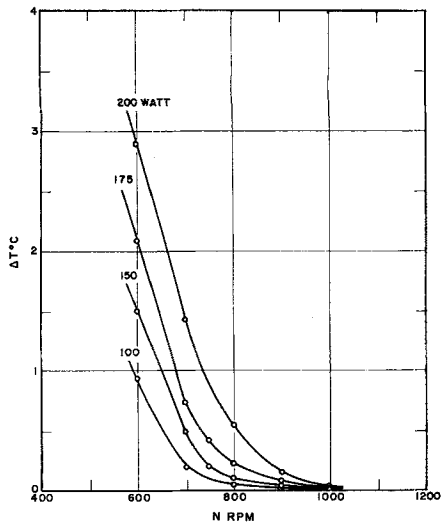

Fig. 2. ΔT vs. N at constant heat load, pentane-water system.

ume) dispersion. The mixer and heater input were set, and once evaporation started, the condenser operated under total reflex. Readings were taken after steady state conditions set in.

Experimental Results

The experiments were confined to a relatively narrow range of heating load (0.29 ÷ 0.57 cal./cc. min.) and mixer Reynolds numbers (3.6×10^4 to 6.0×10^4). The temperature in the cell was found to be uniform and was assumed to be that of the continuous phase only, the temperature gradient being taken as the difference between the measured values and the boiling point of the dispersed pentane. Figure 2 represents the dependence of the temperature difference on the impeller velocity at constant heat loads and Figure 3 the temperature gradient vs. the heat load at constant impeller speeds.

Analysis of Results

Substitution of the appropriate values of a and b estimated from Tables 1 and 2 in Equation (15) for the four-blade paddle used in this work yields

$$\frac{\bar{\epsilon}}{\epsilon_0} = 1 - 12\frac{G}{ND^3} \tag{34}$$

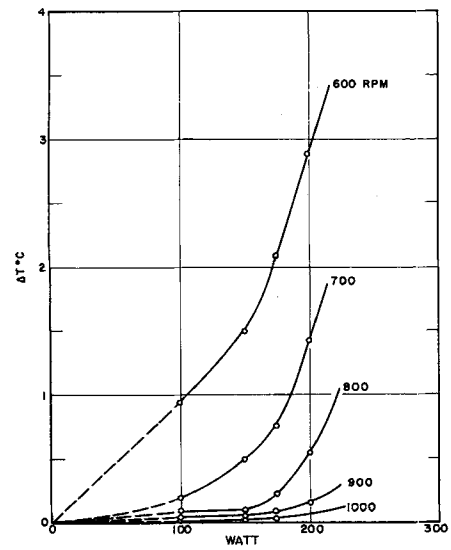

Fig. 3. ΔT vs. q at constant N, pentane-water system.

and, above the flooding point

$$\frac{\bar{\epsilon}}{\epsilon_0} = 0.35 - 1.15\frac{G}{ND^3} \tag{35}$$

Now

$$G = \frac{q_v V}{\rho_G \lambda} \tag{36}$$

where the latent heat of evaporation $\lambda = 85.4$ cal./g., ρ_G (pentane) $= 0.00285$ g./cc. and $V/D^3 = 15.4$. Equations (34) and (35) thus become

$$\frac{\bar{\epsilon}}{\epsilon_0} = 1 - 761\frac{q_v}{N} \tag{37}$$

$$\frac{\bar{\epsilon}}{\epsilon_0} = 0.35 - 73\frac{q_v}{N} \tag{38}$$

The experimental $q_v^{1/6}/\Delta T$ vs. ϵ, calculated by Equations (37) and (38), is plotted in Figure 4, the slope of the straight line (by the least squares method) being 2.0. Hence

$$\frac{q_v^{1/6}}{\Delta T} \sim \bar{\epsilon}^{2.0} \tag{39}$$

Comparison of the exponent (y) in Equations (39) and (33) indicates that the dilute pentane-water system tested is most probably governed by the viscous stress breakup regime, which is consistent with the previously reported work on liquid-gas systems. When one considers all the assumptions made in the derivations, the possible errors involved in estimating the constants a and b as well as in the experimental work, the agreement between the theoretical and experimental results are quite satisfactory. The two corresponding lines are compared in Figure 4.

GENERALIZATION OF PROPOSED CORRELATION

The proposed correlation [Equation (33)] is based on a number of assumptions which may not hold in actual practice. However, it is suggested that by modifying and/or extending some of these assumptions in accordance with practical applications and operating conditions, the general form of the correlation will be retained, namely

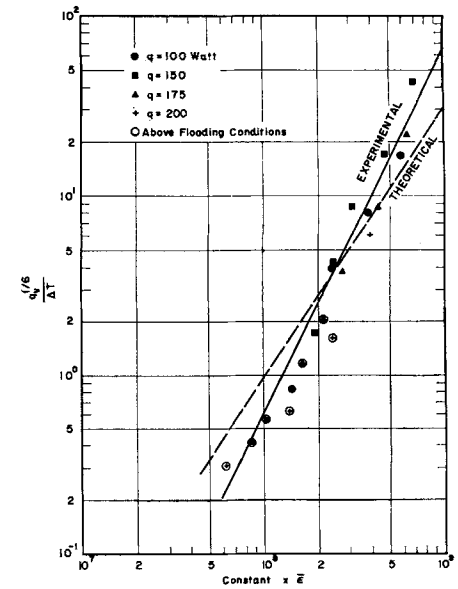

Fig. 4. Experimental $q_v^{1/6}/\Delta T$ vs. calculated $\bar{\epsilon}$ pentane-water system.

$$\frac{q_v^x}{\Delta T} \sim \bar{\epsilon}^y \qquad (40)$$

As is presently shown, the exponents x, y vary with the operating conditions. Some of the practical cases envisaged are as follows.

Case I: $\phi > 5\%$, and particle size is affected by interaction. For this case, substitution of (32) into Equations (13) and (14) yields

$$x = 0.466$$

and

$y = 1.18$ for the viscous regime, $y = 1.08$ for the kinetic regime, and $y = 0.93$ for the coalescence-prevention regime.

Case II: Only partial evaporation takes place in the dispersed phase, and the volatile droplets coalesce into a liquid layer which floats above the continuously agitated fluid. This is the case when energy input is insufficient or the temperature driving force is inadequate, usually when the apparatus is overcharged with the volatile phase.

Assume that the vapor-phase holdup is very small compared with the volatile liquid holdup, the latter being constant, independent of the heat flow rate and power input. Also assume that even under these extreme operating conditions the continuous phase resistance controls the heat transfer phenomena. Accordingly, Equations (13), (14), (20*a*), (29), and (31) yield $x = 1.0$, $y = 0.75$ for the viscous regime (if any), $y = 0.65$ for the kinetic regime, and $y = 0.5$ for the coalescence-prevention regime. [These relationships may be improved by allowing for the internal resistance to heat transfer. Since the latter is also dependent on the Reynolds number (22, 23), a similar relationship is obtained, with x and y then being dependent on the ratio of the internal and external resistance.]

Some pilot plant data from operation under some of the conditions stipulated in Case II are available. The data are plotted in Figure 5 as ΔT vs. q_v at constant power inputs yielding $x = 0.65$, and a plot of $q_v^{0.65}/\Delta T$ vs. $\bar{\epsilon}$ yields $y = 0.25$. When one considers the very rough approximations used in the case, general agreement is, at least, fair. More important, the susceptibility of these extremely different data to this analysis testifies to the general nature of this correlation.

Case III: This is the extreme case where the two liquid phases are completely separated, with the lighter volatile liquid floating above the heavier water phase.

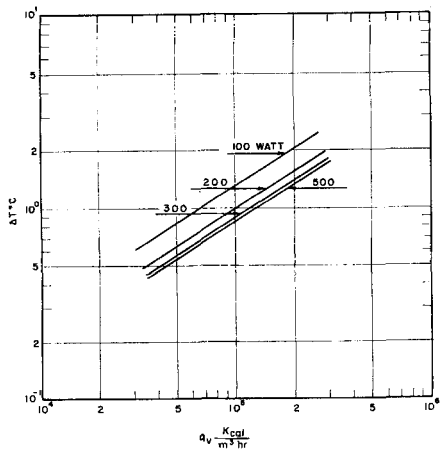

Fig. 5. ΔT vs. q_v at constant energy inputs, pilot plant data.

Under these conditions the concept of local isotropy is no longer applicable. However, $\bar{\epsilon}$ may still be used to represent mixing power input, though the difference is obvious. Experimental evidence (24) indicates that

$$q_A^x/\Delta T \sim \bar{\epsilon}^{0.06} \qquad (41)$$

for $10{,}000 < N_{Re} < 40{,}000$ where $x \simeq 0.7$. Note that q_A, heat flux per unit area replaces q_v in Equation (40). $N_{Re} = ND^2/\nu_c$.

It is interesting to note that up to $N_{Re} = 10^4$ no effect of the mixing is evident, irrespective of the phase in which the process takes place. However, above this Reynolds number the mixing effect on heat transfer is much more pronounced when the mixing takes place in the volatile phase. Higher transfer coefficients were obtained, the smaller the distance of the agitator blades (in the volatile phase) from the liquid-liquid interface. At $N_{Re} > 4 \times 10^4$ the liquid-liquid interface starts to break up with volatile droplets entering the water phase, and the effect of power input becomes much more pronounced.

Case IV: This is the case of low Reynolds numbers ($< 10^4$). At its limit of zero mixing $y = 0$, and Equation (41) reduces to:

$$q_A \sim \Delta T^{1/x} \qquad (42)$$

which is the well-known form of the boiling heat transfer equations, with $1/x = n = 1.25$ representing surface boiling and $1/x = n = 3$ to 4 nucleate boiling. For the pentane-water system in question $n = 1.4$ was obtained, consistent with the observed surface evaporation. A marked increase in n was noted in the presence of artificial nuclei at the liquid-liquid interface. These results are in agreement with the data reported by Gordon et al. (25) for water and alcohols boiling above mercury. The maximum value of n taken from his data is 1.7 obtained for the conditions where the mercury-water interface was quite unstable and interfacial turbulence evident. Thus, the rate of heat transfer increases with increasing interfacial turbulence, irrespective of whether this turbulence is induced by high heat fluxes (as in Gordon's mercury-water system), induced boiling by artificial nucleation sites, or mechanical agitation at the liquid-liquid interface.

CONCLUSIONS

A simple and practical correlation was derived relating energy input, temperature driving force, and heat flow rate for each of the conceivable controlling regimes in a three-phase two-component liquid-liquid vapor system. The usefulness of the derived correlation was demonstrated experimentally for a specific water-pentane system representative of the refrigeration medium in water desalination projects. For this system, with dispersed-phase volumetric holdup of about 5% and complete evaporation of the volatile liquid while still in dispersion, the drop size controlling mechanism is indicated to be breakup by viscous shear stresses. This characteristic is closely related to that of two-phase liquid gas systems. Agreement between the derived correlation and experimental work is satisfactory. The derivation re-emphasizes the well-known risks of scale up of mixing systems without experimental basis. The mixing regime is shown to be characteristic of the system in question and of the operating conditions. The proposed correlation permits convenient and simple experimental determination of the controlling mixing regime.

The generality of the proposed correlation, of the form

$$\frac{q_v^x}{\Delta T} \sim \bar{\epsilon}^y$$

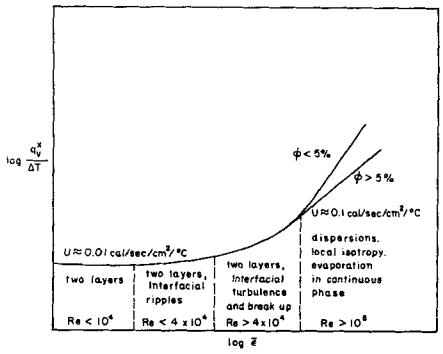

Fig. 6. General representation of the influence of specific power input and turbulence intensity on heat transfer between a nonvolatile liquid and an immiscible, volatile evaporating medium.

is established by modifying and extending some of the underlying specific assumptions in accordance with practical cases and experimental evidence. The range of its applicability is illustrated in Figure 6, indicating the effect of mixing and turbulence intensity on heat transfer between a nonvolatile liquid and an immiscible, volatile, evaporating medium. At the limit of zero external power input the correlation reduces to the well-known boiling correlation, namely

$$q \sim \Delta T^n$$

where the exponent n is shown to vary with the intensity of the interfacial turbulence.

ACKNOWLEDGMENT

The financial support of the Israel National Council for Research and Development is gratefully acknowledged. Thanks are also due to Mr. Arie Golan of the Israel Water Desalinisation Plants (Zarchin) for his continued interest in this work and stimulating discussions, and to Mr. Eliyaho Goldberg for editorial advice.

This work is based in part on the M.Sc. thesis of Zvi Barsky submitted to the Technion in July, 1964.

NOTATION

A = effective liquid-liquid heat transfer area
a = constant, Equation (15)
b = constant, Equation (15)
C = constants, Equations (3) and (4)
C_p = specific heat
D = impeller diameter
d = particle (bubble or droplet) diameter
G = gas flow rate
h = film heat transfer coefficient
k = thermal conductivity
K = equilibrium constant, Equation (5)
L = linear scale of energy containing eddies
m = weight fraction of vapor in evaporating droplet
N = impeller revolutions per unit time
n = exponent, $(= 1/x)$
P = power input
q = heat flow rate
r = distance
T = temperature
t = time
U = overall heat transfer coefficient
u = velocity, relative
V = volume of fluid in mixing tank
v = velocity scale of small energy-dissipation eddy
x = exponent, Equation (40)
y = exponent, Equation (40)

Greek Letters

α = exponent, Equation (17)
β = exponent, Equation (17)
ϵ = energy dissipation per unit mass of fluid
$\bar{\epsilon}$ = average energy dissipation per unit mass of fluid, specific power input
ν = viscosity, kinematic
η = length scale of small energy-dissipation eddy
λ = latent heat of vaporization
μ = viscosity
ρ = density
σ = surface tension
ϕ = holdup, dispersed phase

Subscripts

A = per interfacial unit area
c = continuous phase
d = dispersed phase
G = gas
l = liquid
o = absence of gas
v = per unit volume of fluid

Dimensionless Groups

N_{Re} = Reynolds number $[D^2N/\nu_c]$
N_{We} = Weber number $[\rho N^2 D^3/\sigma]$

LITERATURE CITED

1. Sideman, S., and Y. Taitel, *Intern. J. Heat Mass Trans.*, **7**, 1273 (1964).
2. Shinnar, R., and J. M. Church, *Ind. Eng. Chem.*, **52**, 253 (1960).
3. ———, *J. Fluid Mech.*, **10**, 259 (1961).
4. Kolmogoroff, A. M., *C. R. Acad. Sci. U.S.S.R.*, **30**, 301; **32**, 16 (1941); *Dokl. Akad. Nauk, U.S.S.R.*, **66**, 825 (1949).
5. Aiba, S., *A.I.Ch.E. Journal*, **4**, 487 (1958).
6. Rushton, J. H., E. W. Costich, and H. J. Everett, *Chem. Eng. Progr.*, **46**, 395, 467 (1950).
7. Weiss, L. H., J. L. Fick, R. H. Houston, and T. Vermeulen, *UCRL-9787*, Univ. of California, Berkeley, California (1962).
8. Vermeulen, T., G. M. Williams, and G. E. Langlois, *Chem. Eng. Progr.*, **51**, 85-F (1955).
9. Calderbank, P. H., *Trans. Inst. Chem. Engrs.*, **36**, 443 (1958).
10. Pavlushenko, I. S., and A. V. Yanishevski, *J. Appl. Chem. U.S.S.R.*, **32**, 1529 (1959). In English.
11. Rodrigez, F., L. C. Grotz, and D. L. Engle, *A.I.Ch.E. Journal*, **7**, 663 (1961).
12. Rodger, W. A., V. G. Trice, and J. H. Rushton, *Chem. Eng. Progr.*, **52**, 515 (1956).
13. Calderbank, P. H., *Brit. Chem. Eng.*, **1**, 267 (1956).
14. Cooper, C. A., G. A. Fernstren, and S. A. Miller, *Ind. Eng Chem.*, **36**, 504 (1944).
15. Michel, B. J., and S. H. Miller, *A.I.Ch.E. Journal*, **8**, 262 (1962).
16. Oyama, Y., and K. Endoh, *Chem. Eng. (Japan)*, **19**, 2 (1955).
17. Kalinske, A. A., *Sewage Ind. Wastes*, **27**, 572 (1955).
18. Foust, H. C., D. E. Mack, and J. H. Rushton, *Ind. Eng. Chem.*, **36**, 517 (1944).
19. Sideman, S., and H. Shabtai, *Can. J. Chem. Eng.*, **42**, 107 (June, 1964).
20. Calderbank, P. H., and M. B. Moo-Young, *Chem. Eng. Sci.*, **16**, 39 (1961).
21. Barker, J. J., and R. E. Treybal, *A.I.Ch.E. Journal*, **6**, 289 (1960).
22. Johnson, A. S., and A. E. Hamielec, *ibid.*, 145.
23. Hirsch, G., M.Sc. thesis, Technion-Israel Inst. Technol., Haifa, Israel (1963).
24. Sideman, S., to be published.
25. Gordon, K. F., T. Singh, and E. Y. Weissman, *Intern. J. Heat Mass Trans.*, **3**, 90 (1961).

Manuscript received July 28, 1964; revision received October 12, 1964; paper accepted October 14, 1964. Paper presented at A.I.Ch.E. Houston meeting.